Two electrons in harmonic confinement coupled to light in a cavity

Chenhang Huang, Alexander Ahrens, Matthew Beutel, and Kálmán Varga*
Department of Physics and Astronomy, Vanderbilt University, Nashville, Tennessee 37235, USA

(Received 3 August 2021; revised 12 October 2021; accepted 18 October 2021; published 27 October 2021)

The energy and wave function of a harmonically confined two-electron system coupled to light is calculated by separating the wave functions of the relative and center-of-mass (CM) motions. The relative motion wave function has a known quasianalytical solution. The light only couples to the CM variable and the coupled equation can be solved analytically. The approach works for any coupling strength. Examples of wave functions of light-matter hybrid states are presented.

DOI: 10.1103/PhysRevB.104.165147

I. INTRODUCTION

Analytically or numerically easily solvable systems (e.g., by "exact diagonalization") have always been important test grounds for models and approximations. Recently, there is an intense interest in strongly coupled light-matter systems [1–15]. In these systems, the light-matter coupling cannot be treated perturbatively. The electronic excitations and the photons are superimposed, forming hybrid light-matter excitations. In this regime, there are only a few analytical approaches available to test and develop efficient numerical methods. Reviews of the recent theoretical and experimental development can be found in Refs. [16–18].

In this paper, we consider a two-electron system interacting via the Coulomb interaction, confined by a harmonic oscillator interaction coupled to light in a cavity. The system is described on the level of the Pauli-Fierz (PF) nonrelativistic quantum electrodynamic (QED) Hamiltonian. The two-electron system in harmonic oscillator confinement is a quasiexactly solvable (QES) problem. The wave function can be written as a product of the wave functions of the relative and center-of-mass (CM) motion. The relative motion wave function can be expanded into an infinite series. For certain oscillator parameters, this infinite series can be reduced to a recursion [19]. The wave function of the CM motion is a simple harmonic oscillator eigenfunction. We will show that the photons only couple to the CM coordinate and the coupled CM photon system can be solved exactly using shifted Fock states.

The two-particle systems have long been investigated due to their analytic and quasiexact solvability, which provides straightforward intuition for the physical system under scrutiny as well as an excellent benchmark test for numerical computations. Examples of QES quantum systems are the two-dimensional (2D) harmoniums [19,20] and the hydrogenlike atoms in homogeneous magnetic fields [21]. These QES problems have been generalized to relativistic cases as well [22,23]. For harmonium systems, the separability condition guarantees the quasi-exact solvability for the Schrödinger equation [24], and linearly coupled oscillators have been studied under this condition [25]. For hydrogenlike models, solutions have been found for particular forms of the inhomogeneous magnetic fields [26,27]. Examples of other known QES models include the planar Dirac electron in hydrogenlike atoms [28,29], one-body problems in power-law central potentials [30,31], relativistic 2D pion in constant magnetic fields [32], and 1D and 3D regularized Calogero models [33,34]. QES models with different forms of confinements, e.g., two electrons in one [35] or two [36] 1D rings, two electrons on the surface of the n-sphere (spherium)[37,38], have also been studied.

The exact or even the numerical solution for light-matter coupled systems is very difficult even on the level of a minimal coupling Hamiltonian in the long-wavelength limit [39], because the photons substantially increase the number degrees of freedom of the system. Theoretical approaches have been developed to tame the light-matter coupled systems using approximations and transformations [15,39–48]. In Refs. [41,42], an electron in a 2D potential coupled to a single photon mode is used as a numerical benchmark test. The spatial part of the wave function is represented on a real space grid and coupled to the Fock space of the photons. The Hamiltonian of the system can be diagonalized in this representation and the light coupled wave function can be studied. In Ref. [43], the spatial wave function of the He, HD^+, and H_2^+ three-particle system is represented using a 3D product of pseudospectral basis functions, and a few Fock space states of a single photon mode are coupled to the spatial part. The energy and wave function is calculated by exact diagonalization of the PF Hamiltonian and the Jaynes-Cummings limit for electronic and rovibrational transitions are studied. 1D model systems of atoms and molecules [1,44], often using the Shin-Metiu potential [49], are also useful to describe potential energy surfaces in cavities and test numerical approaches.

The free electron gas also allows analytical treatment [48]. In Ref. [48], the free electron gas in cavity is analytically solved in the long-wavelength limit for an arbitrary number of noninteracting electrons. It is found that the electron-photon ground state is a Fermi liquid containing virtual photons.

*kalman.varga@vanderbilt.edu

Approaches to reformulating the problem have also been proposed. In Ref. [15], the light and matter degrees of freedom are decoupled using a unitary transformation. In the transformed frame, both the light and the matter Hilbert spaces can be truncated systematically to facilitate an efficient solution. In Ref. [7] a variational formulation is developed and the semianalytical formula is derived for the ground and excited state energies.

II. FORMALISM

We consider two particles with positions $\mathbf{r}_1, \mathbf{r}_2$ and charges z_1, z_2. Later we show that an analytical approach only works for $z_1 = z_2$, but it is useful to consider the general case to show the origin of the coupling to the CM. The Hamiltonian of the system is

$$H = H_e + H_{ph} = H_e + H_p + H_{ep} + H_d. \tag{2.1}$$

H_e is the matter Hamiltonian, H_{ph} describes the matter-photon interaction, which is a sum of three terms, the photon Hamiltonian H_p, the matter-photon coupling H_{ep}, and the dipole self-interaction H_d. The electron-photon interaction can be described by using the PF nonrelativistic QED Hamiltonian. The PF Hamiltonian can be rigorously derived [3,6,10,12,50] by applying the Power-Zienau-Woolley gauge transformation [51], with a unitary phase transformation on the minimal coupling $(p \cdot A)$ Hamiltonian in the Coulomb gauge,

$$H_{ph} = \frac{1}{2}\sum_{\alpha=1}^{N_p}\left[p_\alpha^2 + \omega_\alpha^2\left(q_\alpha - \frac{\boldsymbol{\lambda_\alpha}}{\omega_\alpha}\cdot\mathbf{D}\right)^2\right], \tag{2.2}$$

where $\mathbf{D} = \sum_{i=1}^{N} q_i \mathbf{r}_i$ is the dipole operator. The photon fields are described by quantized oscillators. $q_\alpha = \frac{1}{\sqrt{2\omega_\alpha}}(\hat{a}_\alpha^+ + \hat{a}_\alpha)$ is the displacement field and $p_\alpha = -i\sqrt{\frac{\omega_\alpha}{2}}(\hat{a}_\alpha - \hat{a}_\alpha^+)$ is the conjugate momentum. This Hamiltonian describes N_p photon modes with frequency ω_α and coupling $\boldsymbol{\lambda}_\alpha$. The coupling term is usually written as [52]

$$\boldsymbol{\lambda}_\alpha = \sqrt{4\pi}\, S_\alpha(\mathbf{r})\mathbf{e}_\alpha, \tag{2.3}$$

where $S_\alpha(\mathbf{r})$ is the mode function at position $\mathbf{r}$ and $\mathbf{e}_\alpha$ is the transversal polarization vector of the photon modes.

The three components of the electron-photon interaction are as follows: The photonic part is

$$H_p = \sum_{\alpha=1}^{N_p}\left(\frac{1}{2}p_\alpha^2 + \frac{\omega_\alpha^2}{2}q_\alpha^2\right) = \sum_{\alpha=1}^{N_p}\omega_\alpha\left(\hat{a}_\alpha^+\hat{a}_\alpha + \frac{1}{2}\right). \tag{2.4}$$

By using the creation and annihilation operators, the photon states $|n_\alpha\rangle$ can be generated by multiple applications of the creation operators on the vacuum state $|n_\alpha\rangle = (\hat{a}_\alpha^+)^n|0\rangle$. All other photon operations can be done by using $\hat{a}_\alpha$ and $\hat{a}_\alpha^+$. The interaction term is

$$H_{ep} = -\sum_{\alpha=1}^{N_p}\omega_\alpha q_\alpha \boldsymbol{\lambda_\alpha}\cdot\mathbf{D} = -\sum_{\alpha=1}^{N_p}\sqrt{\frac{\omega_\alpha}{2}}(\hat{a}_\alpha + \hat{a}_\alpha^+)\boldsymbol{\lambda_\alpha}\cdot\mathbf{D}. \tag{2.5}$$

Only photon states $|n_\alpha\rangle$, $|n_\alpha \pm 1\rangle$ are connected by $\hat{a}_\alpha$ and $\hat{a}_\alpha^+$. The matrix elements of the dipole operator $\mathbf{D}$ are only nonzero between spatial basis functions with angular momentum l and $l \pm 1$ in 3D or m and $m \pm 1$ in2D. The strength of the electron-photon interaction can be characterized by the effective coupling parameter

$$g_\alpha = |\boldsymbol{\lambda_\alpha}|\sqrt{\frac{\omega_\alpha}{2}}. \tag{2.6}$$

The dipole self-interaction is

$$H_d = \frac{1}{2}\sum_{\alpha=1}^{N_p}(\boldsymbol{\lambda_\alpha}\cdot\mathbf{D})^2, \tag{2.7}$$

which describes the effects of the polarization of the matter back on the photon field. The importance of this term for the existence of a ground state is discussed in Ref. [6].

A. Separation of the relative and center of mass equations

For simplicity we only consider a single photon mode. The formalism can be easily extended to many photon modes as described in Appendix B and Appendix C. We will define the coupling strength as $\boldsymbol{\lambda} = (\lambda, \lambda, 0)$. A more general case is described in Appendix C. In this section, we consider the Hamiltonian that acts only in the matter space

$$H_e + H_d = -\frac{1}{2}\nabla_1^2 + \frac{1}{2}\omega_0^2\mathbf{r}_1^2 - \frac{1}{2}\nabla_2^2 + \frac{1}{2}\omega_0^2\mathbf{r}_2^2 + \frac{z_1 z_2}{|\mathbf{r}_1 - \mathbf{r}_2|} + \frac{1}{2}(z_1\boldsymbol{\lambda}\cdot\mathbf{r}_1 + z_2\boldsymbol{\lambda}\cdot\mathbf{r}_2)^2. \tag{2.8}$$

Atomic units $\hbar = m = e = 1$ are used throughout and unit charges are assumed.

Defining relative and CM coordinates as

$$\begin{aligned}\mathbf{r} &= \mathbf{r}_2 - \mathbf{r}_1,\\ \mathbf{R} &= \tfrac{1}{2}(\mathbf{r}_1 + \mathbf{r}_2),\end{aligned} \tag{2.9}$$

the Hamiltonian decouples into a relative and CM Hamiltonian

$$\begin{aligned}H_e + H_d &= -\nabla_{\mathbf{r}}^2 + \frac{1}{4}\omega_0^2\mathbf{r}^2 + \frac{z_1 z_2}{r} - \frac{1}{4}\nabla_{\mathbf{R}}^2 + \omega_0^2\mathbf{R}^2 + \frac{1}{2}\left(\boldsymbol{\lambda}\cdot\left((z_1+z_2)\mathbf{R} + \frac{1}{2}(z_1 - z_2)\mathbf{r}\right)\right)^2\\ &\equiv H_{\mathbf{r}} + H_{\mathbf{R}},\end{aligned} \tag{2.10}$$

and the corresponding eigenvalue problem is

$$(H_{\mathbf{r}} + H_{\mathbf{R}})\Phi(\mathbf{r}, \mathbf{R}) = (\epsilon + \eta)\Phi(\mathbf{r}, \mathbf{R}), \tag{2.11}$$

and $E = \epsilon + \eta$ is the eigenenergy. Note that there is no cross term between $\mathbf{R}$ and $\mathbf{r}$. For like charges, the last term only contributes to $H_{\mathbf{R}}$, and for opposite charges it only contributes to $H_{\mathbf{r}}$.

1. $z_1 = -z_2$

In this case the photon only couples to $\mathbf{r} = (x, y, z)$. The CM wave function is a harmonic oscillator eigenfunction with frequency $2\omega_0$. By introducing $u = \frac{x+y}{\sqrt{2}}$, and $v = \frac{-x+y}{\sqrt{2}}$, the relative motion Hamiltonian takes the form

$$H_{\mathbf{r}} = -\nabla_u^2 - \nabla_v^2 - \nabla_z^2 + \frac{1}{2}\omega_u^2 u^2 + \frac{1}{2}\omega_v^2 v^2 + \frac{1}{2}\omega_z^2 z^2 - \frac{1}{(u^2 + v^2 + z^2)^{1/2}}, \tag{2.12}$$

where $\omega_u{}^2 = 2\lambda^2 + \frac{1}{2}\omega_0{}^2$, $\omega_v{}^2 = \omega_z{}^2 = \frac{1}{2}\omega_0{}^2$. This is a single particle Coulomb problem in an anisotropic harmonic potential. The derivation is detailed in the next section. We are not aware of any existing analytical solutions to this system. One can, in principle, solve this problem using a product basis of the $u - v - z$ harmonic oscillators, but we do not pursue this case any further in this paper.

2. $z_1 = z_2$

In the following, we will consider $z_1 = z_2$ because, in this case, the equation for the relative motion can be analytically found for certain frequencies as mentioned before. After multiplying the relative part by $1/2$ and the CM part by 2 to bring the equations in a more convenient form, we have

$$\left[-\frac{1}{2}\nabla_{\mathbf{r}}^2 + \frac{1}{2}\omega_{\mathbf{r}}^2\mathbf{r}^2 + \frac{1}{2}\frac{1}{r}\right]\varphi(\mathbf{r}) = \varepsilon'\varphi(\mathbf{r}), \tag{2.13}$$

where $\omega_{\mathrm{r}} = \frac{1}{2}\omega_0$ and $\varepsilon' = \frac{1}{2}\varepsilon$, and

$$\left[-\tfrac{1}{2}\nabla_{\mathbf{R}}^2 + \tfrac{1}{2}\omega_{\mathbf{R}}^2\mathbf{R}^2 + 4(\boldsymbol{\lambda}\cdot\mathbf{R})^2\right]\xi(\mathbf{R}) = \eta'\xi(\mathbf{R}), \tag{2.14}$$

where $\omega_{\mathbf{R}} = 2\omega_0$ and $\eta' = 2\eta$. The total wave function can be written as

$$\Phi(\mathbf{r},\mathbf{R}) = \varphi(\mathbf{r})\xi(\mathbf{R}). \tag{2.15}$$

In this case, the CM motion in the z direction is described by a harmonic oscillator eigenfunction, and we drop this part for now.

In 2D, using $\mathbf{R} = (X, Y)$ one can rewrite $H_{\mathbf{R}}$ as (in 3D one simply has to multiply the CM wave function with a harmonic oscillator function of frequency $2\omega_0$ in the Z direction)

$$H_{\mathbf{R}} = -\frac{1}{2}\frac{\partial^2}{\partial X^2} - \frac{1}{2}\frac{\partial^2}{\partial Y^2} + \frac{1}{2}\omega_X^2X^2 + \frac{1}{2}\omega_Y^2Y^2 + \frac{1}{2}\omega_{XY}^2XY, \tag{2.16}$$

where

$$\omega_X^2 = \omega_Y^2 = \omega_{\mathbf{R}}^2 + 8\lambda^2, \quad \omega_{XY}^2 = 16\lambda^2. \tag{2.17}$$

Using a unitary transformation (a generalized version is presented in Appendix B)

$$U = \frac{X+Y}{\sqrt{2}}, \quad V = \frac{-X+Y}{\sqrt{2}}, \tag{2.18}$$

we have

$$\begin{aligned} H_{\mathbf{R}} &= -\frac{1}{2}\frac{\partial^2}{\partial U^2} - \frac{1}{2}\frac{\partial^2}{\partial V^2} + \frac{1}{2}\omega_U^2U^2 + \frac{1}{2}\omega_V^2V^2 \\ &\equiv H_U + H_V, \end{aligned} \tag{2.19}$$

where

$$\omega_U^2 = \tfrac{1}{2}\left(\omega_X^2 + \omega_{XY}^2 + \omega_Y^2\right) = \omega_R^2 + 16\lambda^2, \tag{2.20}$$

$$\omega_V^2 = \tfrac{1}{2}\left(\omega_X^2 - \omega_{XY}^2 + \omega_Y^2\right) = \omega_R^2. \tag{2.21}$$

This Hamiltonian is analytically solvable: the lowest energy is

$$\eta = \frac{1}{2}\left(\omega_0 + \sqrt{\omega_0^2 + 4\lambda^2}\right). \tag{2.22}$$

$H_{\mathbf{r}}$ is also analytically solvable, in this case, for certain frequencies [19,53]. For example, for $\omega_0 = 1$ one gets $\epsilon = 2$ (see the Table in Ref. [53]) and the total energy is $E = 2 + \frac{1}{2} + \frac{1}{2}\sqrt{1+4\lambda^2}$.

The Hamiltonian in Eq. (2.14) is multiplied by 2. To return the the normal Hamiltonian one has to define

$$u = \sqrt{2}U, \quad v = \sqrt{2}V, \quad \omega_u = \frac{\omega_U}{2}, \quad \omega_v = \frac{\omega_V}{2} \tag{2.23}$$

and

$$H_u = -\frac{1}{2}\frac{\partial^2}{\partial u^2} + \frac{1}{2}\omega_u^2, \quad H_v = -\frac{1}{2}\frac{\partial^2}{\partial v^2} + \frac{1}{2}\omega_v^2. \tag{2.24}$$

With these transformations $H_U = 2H_u$ and $H_V = 2H_v$, and H_u and H_v will be used from now. The wave function of the CM motion now can be written as

$$\xi(\mathbf{R}) = \phi_k(u)\phi_l(v), \tag{2.25}$$

where ϕ_k is the kth eigenfunction of the one-dimensional harmonic oscillator,

$$\phi_k(u) = \left(\frac{\sqrt{\omega_u}}{\sqrt{\pi}\,2^k k!}\right)^{\frac{1}{2}} \mathrm{e}^{-\frac{\omega_u}{2}u^2} H_k(\sqrt{\omega_u}\,u), \tag{2.26}$$

where H_k is the Hermite polynomial. The eigenfunctions are defined similarly for v.

B. Photon-electron coupling

For a single photon mode, the coupling term Eq. (2.5) takes the form

$$H_{ep} = -\sqrt{\frac{\omega}{2}}(\hat{a} + \hat{a}^+)\lambda D = -\omega q \lambda D, \quad D = 2u \tag{2.27}$$

so only the u harmonic oscillators are coupled with photons. The Hamiltonian that we have to solve is reduced to a single one-dimensional electronic Hamiltonian coupled to light:

$$H_c = H_u + H_p - 2\omega\lambda q u, \tag{2.28}$$

where H_p is defined in Eq. (2.4). In the above Hamiltonian the eigenstates of the CM Hamiltonian are the $\phi_k(u)$ harmonic oscillator eigenfunctions, the eigenstates of $H_p = \omega(\hat{a}^+\hat{a} + \frac{1}{2})$ are the photon Fock states $|n\rangle$, and the last term couples the CM and photon harmonic oscillators.

The Hamiltonian in Eq. (2.28) can be diagonalized in two different ways. In the first approach, new variables are introduced to decouple the CM and photon harmonic oscillators [54], in the second one a product basis of the CM and photon harmonic oscillators, $\phi_k(u)|n\rangle$ is used. The advantage of the first approach is that it is exact, while numerical diagonalization is needed in the second approach. The advantage of the second approach is that the solution is directly obtained as a product of spatial and photon spaces.

1. Shifted Fock states

By introducing the coordinate rotation

$$s = u\sin(\alpha) + q\cos(\alpha), \tag{2.29}$$

and

$$t = -u\cos(\alpha) + q\sin(\alpha), \tag{2.30}$$

the coupling term in Eq. (2.28) can be eliminated by choosing

$$\tan(2\alpha) = \frac{4\omega\lambda}{\chi}, \quad \chi = \omega_u^2 - \omega^2, \tag{2.31}$$

where $\omega_u^2 = \omega_0^2 + 4\lambda^2$. The Hamiltonian in Eq. (2.28) becomes

$$H_c = -\frac{1}{2}\frac{\partial^2}{\partial s^2} + \frac{1}{2}\omega_s^2 s^2 - \frac{1}{2}\frac{\partial^2}{\partial t^2} + \frac{1}{2}\omega_t^2 t^2, \tag{2.32}$$

where

$$\omega_s = |\sin\alpha|\sqrt{\omega_0^2 + (2\lambda - \omega/\tan\alpha)^2}, \tag{2.33}$$

$$\omega_t = |\cos\alpha|\sqrt{\omega_0^2 + (2\lambda + \omega\tan\alpha)^2}. \tag{2.34}$$

The energy spectrum of H_c is

$$E(n_s, n_t) = \left(n_s + \tfrac{1}{2}\right)\omega_s + \left(n_t + \tfrac{1}{2}\right)\omega_t, \tag{2.35}$$

and the eigenfunction is

$$\phi_{n_s n_t}(s,t) = \phi_{n_s}(s)\phi_{n_t}(t). \tag{2.36}$$

Note that the arguments of the harmonic oscillator functions are now coupled light-matter coordinates, shifted Fock states [41]. One can rewrite these as products of spatial variables and photon Fock spaces by expanding the harmonic oscillator functions. The next section shows a different solution which gives the results directly as a product of CM harmonic oscillators and photon states. The results of this section is generalized for multiphoton modes in Appendix A.

To study the dependence of ω_s and ω_t on ω we first consider the cases when the numerator or the denominator is zero in Eq. (2.31). In the first case, $\omega = 0$ and $\alpha = 0$, therefore

$$\omega_s = 0, \quad \omega_t = \omega_u. \tag{2.37}$$

There is no coupling so we get back the CM harmonic oscillator, but the important thing is that we know that ω_s starts from zero. If the denominator is zero, $\chi \approx 0$,

$$\omega \approx \omega_u = \sqrt{\omega_0^2 + 4\lambda^2} \tag{2.38}$$

and we have two limiting cases. If $\chi \to 0_+$ then $\alpha \to \pi/4$ and

$$\omega_s = \omega\sqrt{1 - 2\lambda/\omega}, \tag{2.39}$$

$$\omega_t = \omega\sqrt{1 + 2\lambda/\omega}, \tag{2.40}$$

and if $\chi \to 0_-$ then $\alpha \to -\pi/4$ and

$$\omega_s = \omega\sqrt{1 + 2\lambda/\omega}, \tag{2.41}$$

$$\omega_t = \omega\sqrt{1 - 2\lambda/\omega}, \tag{2.42}$$

note that the frequencies are real Eq. (2.38). This shows that there is a discontinuity at $\omega = \omega_u$ and ω_s and ω_t are ω_s and ω_t are swapped at this frequency. It is also clear from Eq. (2.38) that for a given confinement and coupling strength this transition always exists for a suitable ω.

The transition occurs at ω_u which is the characteristic frequency of the CM motion. If the coupling strength is weak, then $\omega_u \approx \omega_0$ and the transition frequency is determined by the confinement alone. In this case the system behaves like a multilevel Jaynes-Cummings model, where the atomic energy levels (now harmonic oscillator levels) define the transition. To show this we introduce $x = \lambda/\sqrt{\omega}$ so that the coupling is as Eq. (2.27) shows proportional to $g = \omega$ as in the Jaynes-Cummings model. Now Eq. (2.31) can be written as

$$\tan(2\alpha) = \frac{4\omega^{3/2}x}{\omega_0^2 + (4x^2 - 1)\omega^2}. \tag{2.43}$$

If $x > 0.5$ then right-hand side is positive for any ω and there is no transition (this does not happen in the previously discussed general case because there ω and λ are independent). If $x < 0.5$ then there is a transition and if $x \ll 1$ ($\lambda \ll 1$) then the transition happens at the energy level difference of the harmonic oscillator, $\omega \approx \omega_0$. Figure 1(a) shows ω_s and ω_t for $x = 1/10$ and $\omega_0 = 0.5$. At $\omega \approx \omega_0$ the lower frequency mode, ω_s, becomes the higher frequency mode, and the higher frequency ω_t mode becomes the lower frequency mode. The transition energy (Rabi splitting) is

$$\Omega = 2\lambda. \tag{2.44}$$

Figure 1(b) shows the energies, $E(n_s, n_t)$, for $n_t + n_s \leqslant 3$. Transition occurs between (n_t, n_s) and (n_s, n_t) states when $n_t \neq n_s$.

2. *Exact diagonalization*

The Hamiltonian in Eq. (2.28) can also be solved by exact diagonalization using the product of center of mass eigenfunctions and photon Fock states as basis states

$$\phi_k(u)|n\rangle. \tag{2.45}$$

For the diagonalization, one needs the matrix elements of the Hamiltonian which are readily available. The operators H_u and u act on the real space, and $\hat{a} + \hat{a}^+$ acts on the photon space. For the coupling term in the photon space:

$$\begin{aligned} q|n\rangle &= \frac{1}{\sqrt{2\omega}}(\hat{a} + \hat{a}^+)|n\rangle \\ &= \frac{1}{\sqrt{2\omega}}\left(|\sqrt{n}|n-1\rangle + \sqrt{n+1}|n+1\rangle\right), \end{aligned} \tag{2.46}$$

and the matrix elements of q are

$$\langle m|q|n\rangle = \frac{1}{\sqrt{2\omega}}D_{mn}, \tag{2.47}$$

where

$$D_{mn} = \begin{pmatrix} 0 & \sqrt{1} & 0 & 0 & 0 & \dots \\ \sqrt{1} & 0 & \sqrt{2} & 0 & 0 & \dots \\ 0 & \sqrt{2} & 0 & \sqrt{3} & 0 & \dots \\ 0 & 0 & \sqrt{3} & 0 & \sqrt{4} & \dots \\ 0 & 0 & 0 & \sqrt{4} & 0 & \dots \\ \vdots & \vdots & \vdots & \vdots & \vdots & \ddots \end{pmatrix}. \tag{2.48}$$

The Hamiltonian H_u is diagonal in the harmonic oscillator bases

$$\langle\phi_i|H_u|\phi_j\rangle = \left(j + \tfrac{1}{2}\right)\omega_u\delta_{ij}. \tag{2.49}$$

The matrix elements of the photon Hamiltonian are

$$\langle n|\omega\left(\hat{a}^+\hat{a} + \tfrac{1}{2}\right)|m\rangle = \left(n + \tfrac{1}{2}\right)\omega\delta_{nm}. \tag{2.50}$$

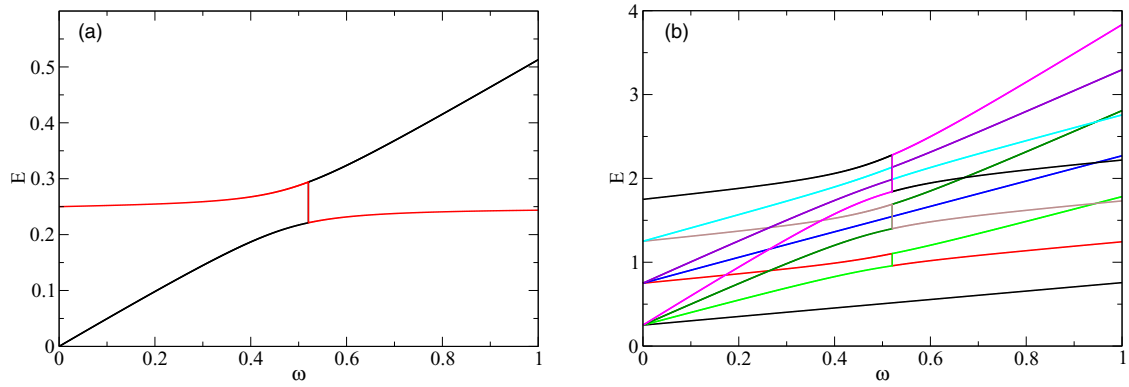

FIG. 1. (a) Frequencies of the eigensolutions of Eq. (2.32) as a function of photon frequency; ω_s (black curve starts at zero at $\omega = 0$) and ω_t (red curve) for $x = 1/10$. (b) The lowest eigenstates of H_c with $n_s + n_t \leqslant 3$ for $x = 10$. The lowest transition is between states $(n_s = 0, n_t = 1)$ and $(n_s = 1, n_t = 0)$ at $\omega = \omega_0$ with energy gap Ω. Next, in the middle, there is a transition between the $(0, 2)$ and $(2, 0)$ states with energy gap 2Ω. In the top, there is a transition between states $(0, 3)$ and $(3, 0)$ with 3Ω and between states $(2, 1)$ and $(1, 2)$ with energy gap Ω.

The last piece is the matrix elements of the position operator in harmonic oscillator bases:

$$\langle \phi_i | u | \phi_j \rangle = \frac{1}{\sqrt{2\omega_u}} D_{ij}. \tag{2.51}$$

Thus, the matrix elements of H_c are

$$\langle m, \phi_i | H_c | n, \phi_j \rangle = \delta_{mn}\delta_{ij}\left(j + \tfrac{1}{2}\right)\frac{\omega_u}{2} + \delta_{mn}\delta_{ij}\left(n + \tfrac{1}{2}\right)\omega + \sqrt{\frac{2\omega}{\omega_u}}\,\lambda\, D_{mn} D_{ij}. \tag{2.52}$$

This is a very sparse matrix and can be diagonalized with sparse matrix approaches even for very large dimensions. In practice, a few dozen photon bases $|n\rangle$ and harmonic oscillator bases ϕ_i give converged energies. This matrix is generalized for N_p photon modes in Appendix B.

After the diagonalization, we have the eigenenergies η_j and the eigenfunctions. The spatial part of the eigenfunctions is a linear combinations of the product of basis functions

$$\psi_j(\mathbf{R}) = \phi_0(v)\phi_j(u), \tag{2.53}$$

and the eigenfunction for the CM motion is

$$\xi_k(\mathbf{R}) = \sum_{n=0}^{K_n}\left(\sum_{j=0}^{K_u} c_{j,n}^k \psi_j(\mathbf{R})\right)|n\rangle = \sum_{j=0}^{K_u}\left(\sum_{n=0}^{K_n} c_{j,n}^k |n\rangle\right)\psi_j(\mathbf{R}), \tag{2.54}$$

where K_u and K_n are some suitably chosen upper limits that control the convergence of the eigenvalues. For the v part of the CM motion, we have chosen the lowest state. The first line in Eq. (2.54) emphasizes the coupling of the spatial part to photon spaces; the second line emphasizes the coupling of the linear combination of photon states to a given CM eigenfunction.

III. RESULTS AND DISCUSSION

In this section we present results using the exact diagonalization approach. The analytical and numerical diagonalization results are in perfect agreement if the basis dimension is sufficiently high. We use the exact diagonalization approach in this section because it gives the result directly in the product of coordinate and photon space.

For the calculations, we have picked an oscillator frequency ω_0 from the Table of Ref. [53], calculated the radial part of the relative wave function as described in Refs. [19,20,53], and multiplied it with the corresponding spherical function. This function is then multiplied by $\xi_k(\mathbf{R})$ calculated using Eq. (2.54).

The wave function can be decomposed into spatial and photon components. The spatial part can be decomposed further into different CM excitations. In the following we explore the wave function components in these subspaces.

First, we show the wave functions for different CM excitations. In this case, two variables determine the behavior: the confining strength ω_0 and the coupling parameter λ. We show 2D examples because it is easier to visualize the electron density in 2D. The 3D cases are very similar, with the only difference being that the wave function is multiplied by the lowest harmonic oscillator function with frequency $2\omega_0$ in the z direction.

A. Spin singlet case

We start with the spin-singlet case with confinement strength $\omega_0 = 1$. The energy of the relative motion in this case is $\epsilon = 1$ a.u. (see the Table in Ref. [53]). The eigenstate with the $j = 0$ harmonic oscillator CM wave function is spherically symmetric for small λ [$lambda = 0.5$, Fig. 2(a)]. For larger λ, ($\lambda = 2$), the anharmonicity of the CM harmonic oscillators dominates ($\omega_v << \omega_u$) and a slightly ellipsoidal structure appears [Fig. 2(b)]. For $j = 1$, the CM state is multiplied by u ($H_1(\sqrt{\omega_u}\,u) = 2\sqrt{\omega_u}\,u$) and it becomes elongated in the diagonal direction [Fig. 2(c)]. This direction is set by the choice of $\boldsymbol{\lambda} = (\lambda, \lambda)$, and other choices would simply

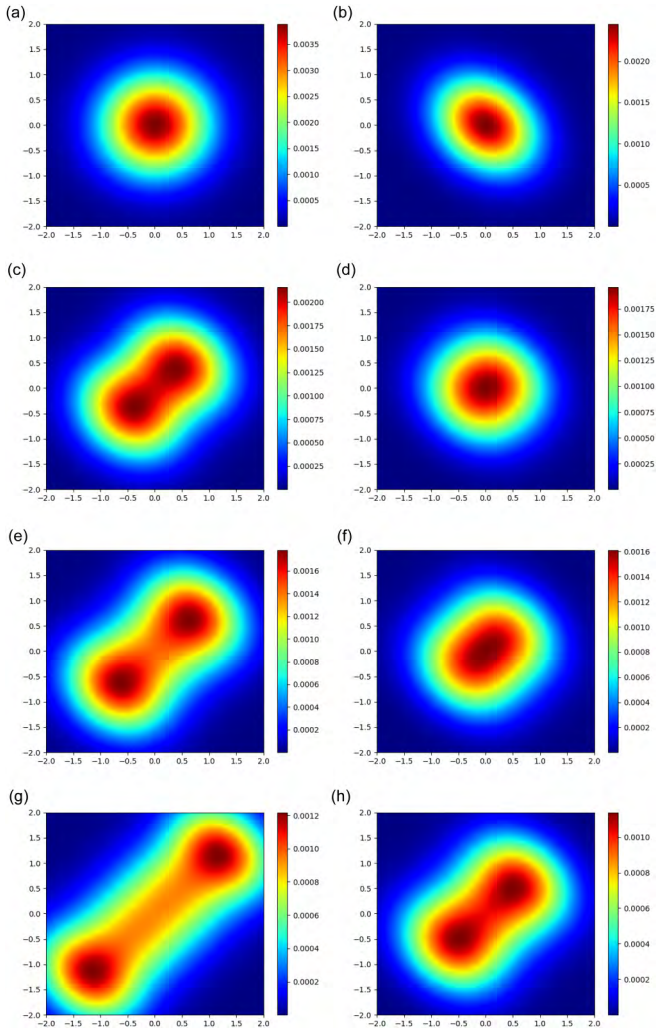

FIG. 2. Two-dimensional electron densities of two electrons confined in a harmonic potential with $\omega_0 = 1$, $\omega = 0.5$ a.u. and spin $S = 0$ for different j (CM quantum number) and λ values. First row: $j = 0$, (a) $\lambda = 0.5$, (b) $\lambda = 2$. Second row: $j = 1$, (c) $\lambda = 0.5$, (d) $\lambda = 2$. Third row: $j = 2$, (e) $\lambda = 0.5$, (f) $\lambda = 2$. Fourth row: $j = 5$, (g) $\lambda = 0.5$, (h) $\lambda = 2$. The x axis is the horizontal, the y axis is the vertical direction. The color bar shows the probability.

change the direction (see Appendix B). For larger λ value, the confinement by ω_u is much stronger and the elongation disappears [Fig. 2(d)]. For higher j values the elongation increases due to the higher order $H_j(\sqrt{\omega_u}u)$ polynomials [Figs. 2(e) and 2(g)]. Higher λ values decrease the elongation [Figs. 2(f) and 2(h)] because the confinement is stronger. This trend continues for even higher j values as well. Solutions with other ω_0 values show very similar behaviors.

Figure 3 shows the singlet state energy spectrum as a function of photon frequency ω. The ground state energy is 3 a.u. in this case. Infinitely many photon states and infinitely many CM states can couple to this state. Without coupling of the photons to the center of mass, the energy of the photon states increases linearly with ω and the energy of the CM states increases linearly with ω_u. Figure 3 shows the lowest 30 states. The coupling is defined as $\lambda = x\sqrt{\omega}$. For $x = 1$ [Fig. 3(a)], some states (primarily photon states) move linearly up with ω for small frequencies, while other states (primarily CM states) only slowly increase with ω. Now we repeat the same calculation as in Sec. II B 1 (shown in Fig. 1) with the CM photon product states. Figure 3(b) shows the energy spectrum. There are many more lines in Fig. 3(b) than in Fig. 1(b) because each CM states is coupled with many photon states. The lowest two states are the same in Figs. 1(b) and 3(b). Then one can see the first transition (note that the transition is shown with a vertical line but there is no swapping between the two states in this case). In this transition case, the lower curve starts at $E = \frac{1}{2}\omega_0$ and the upper curve starts at $E = \frac{3}{2}\omega_0$ in Fig. 1(b). This is also true in Fig. 3(b), but now there are many energy levels (those are raising photon replica states) intersect the path. Figure 3(b). also shows the other transitions presented in Fig. 1(b) with a vertical line in the sea of the photon replica states. This calculation also shows that the analytical shifted Fock states and the numerical diagonalization gives the same result.

To calculate the full energy spectrum of the system, one has to include the excited states of the relative motion. As those states are orthogonal, the complete spectrum can be obtained by shifting the energy levels in Fig. 3 by the energies of the excited states.

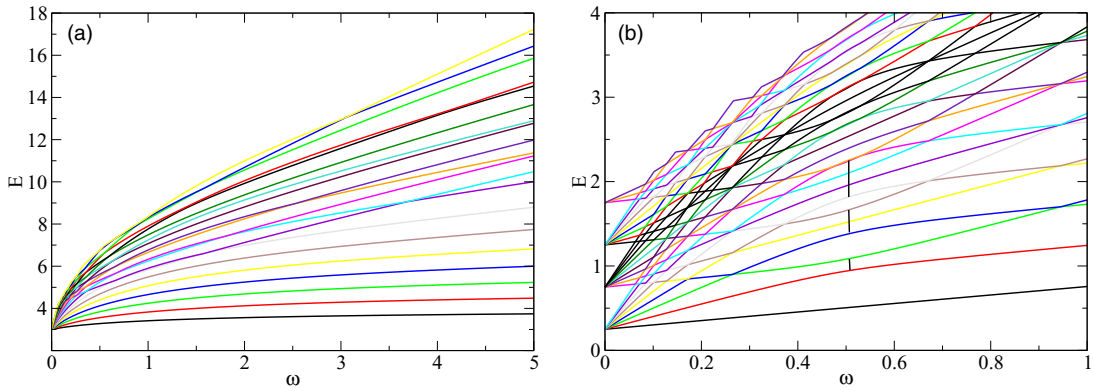

FIG. 3. The energy levels as a function of ω for different λ values (the confinement strength is $\omega_0 = 0.5$ a.u.): (a) $\lambda = \sqrt{\omega}$ and (b) $\lambda = \sqrt{\omega}/10$. The energy of the relative motion is added to the energy in (a), but not in (b) so that (b) can be compared to Fig. 1(b).

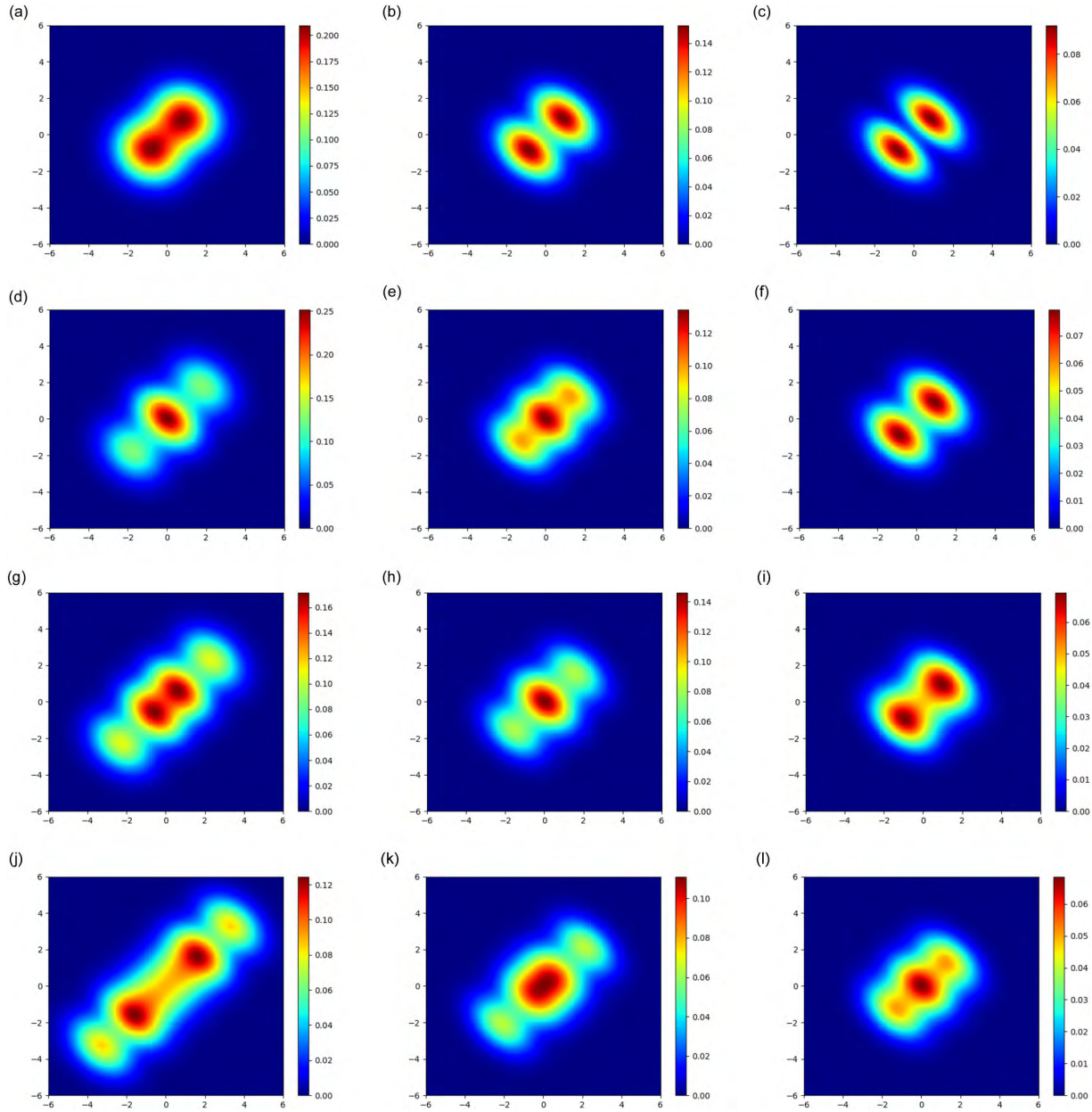

FIG. 4. Two-dimensional densities of two electrons confined by a harmonic potential with $\omega_0 = 1/3$, $\omega = 0.5$ a.u. and spin $S = 1$. for different j (CM quantum number) and λ values. First row: $j = 0$, (a) $\lambda = 0.01$, (b) $\lambda = 0.5$, (c) $\lambda = 2$. Second row: $j = 1$, (d) $\lambda = 0.01$, (e) $\lambda = 0.5$, (f) $\lambda = 2$. Third row: $j = 2$, (g) $\lambda = 0.01$, (h) $\lambda = 0.5$, (i) $\lambda = 2$. Fourth row: $j = 5$, (j) $\lambda = 0.01$, (k) $\lambda = 0.5$, (l) $\lambda = 2$. The x axis is the horizontal, the y axis is the vertical direction. The color bar shows the probability.

B. Spin-triplet case

In the spin-triplet case in 2D we choose $\omega_0 = 1/3$ a.u., and the energy of the relative motion is $\epsilon = 1$ a.u. in this case. Figure 4 shows the densities of the spin-triplet configiration. This system is more sensitive to the choice of λ and we use three different λ values (0.01, 0.5, 2) to illustrate the differences. In the spin-triplet case, the spin function is symmetric, and the spatial part is antisymmetric ($m = \pm 1$ in Eq. (1.2) in Ref. [53]). Two peaks appear in the electron density plot for $j = 0$ as shown in Figs. 4(a), 4(b), and 4(c). By increasing λ the CM u oscillator squeezes the electrons closer to each other but due to the repulsion the separation between the two peaks is more visible (the density between the peaks being lower). There are three peaks for $j = 1$ for $\lambda = 0.01$ and $\lambda = 0.5$, but as the u confinement gets stronger the two peak structure returns [Figs. 4(d), 4(e), and 4(f)]. The three-peak structure is a nontrivial case because, unlike the simple spherical structure in the singlet state, the relative motion function, in this case, is in an $m = 1$ angular momentum state and it is multiplied by u.

For higher j states, the elongation caused by H_j continues [see Figs. 4(g) and 4(j)], and the nodal structure of H_j also contributes to the structure of the density. Overall it seems that the $\lambda = 0.01$ case captures the general trend very well. For larger λ values the same structures appear later as j increases.

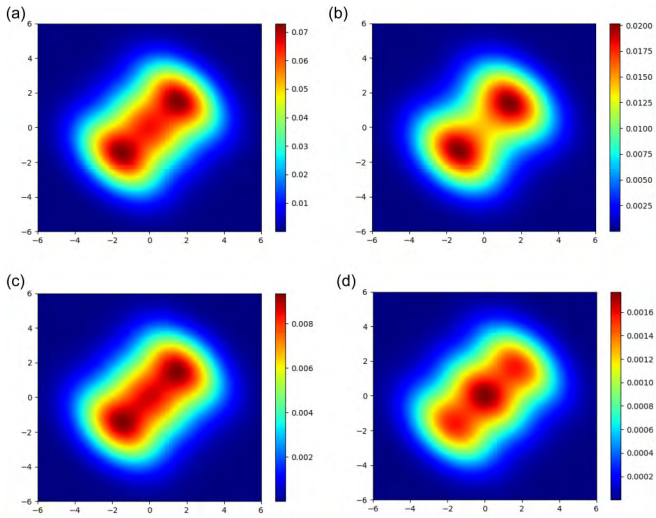

FIG. 5. Two-dimensional electron densities for the $S = 1$ case ($\omega_0 = 0.18055$ a.u., $\omega = 1$ a.u. and $\lambda = 1$ a.u.) in different photon subspaces: (a) total density, (b) density in the $n = 1$ space, (c) density in the $n = 3$ space, (d) density in the $n = 5$ space. The x axis is the horizontal, the y axis is the vertical direction. The color bar shows the probability.

For a given j, increasing λ squeezes the elongation due to the CM ω_u confinement, as in the singlet case.

The wave function of the system will be a linear combination of wave functions shown in Figs. 2 and 4, with coefficients defined in the second line of Eq. (2.54). These coefficients depend on the values of ω, ω_0, and λ. For a single photon mode, the lowest CM harmonic oscillator states often dominate and it is hard to pick parameters that favor a single j CM mode or higher j values. In Fig. 5(a) we present an example for the triplet case where the square of the linear coefficients are 0.55, 0.18, 0.10, 0.06, 0.04, 0.03 ($j = 0, ...5$), so a few $j \neq 0$ contribute to the density. Figures 5(b), 5(c), and 5(d) show the square of the wave function in the $n = 1, 3$ and 5 spaces. The $n = 0$ density is very similar to Fig. 4(b). The squares of the linear coefficients in n space are 0.49, 0.13, 0.11, 0.07, 0.05 ($n = 0, ..., 5$). This example shows that the spatial wave functions in different photon subspaces can be very different and quantum mechanical methods have to look for accurate wave functions in different photon spaces.

The calculations can be extended to more than one photons modes. Examples are shown in Appendix D

IV. SUMMARY

In a harmonically confined two-electron system, the light couples to the dipole moment which is proportional to the CM coordinate. By separating the relative and CM motion, we have shown that the coupled photon CM system can be solved analytically using shifted Fock states and the relative motion part has analytical solutions for certain frequencies. We have also presented a solution which is based on a product of CM harmonic oscillator states and photon states. Using the three main variables of the problem, the frequency of light, the strength of the confinement and the coupling one can define the frequency of the transition between states and the energy difference at the transition frequency. This may be useful in experiments designing two level systems for quantum information processing.

The coupling of the light to the CM coordinate leads to elongated wave functions. The symmetry axis of the electron density is determined by the polarization direction. The density has several peaks depending on the CM excitation and the symmetry axis of the density. The competition between the confinement due to the coupling to light and the node structure of the CM excitation influences the location of the density peaks.

We have shown that the spatial wave functions belonging to different photon spaces are very different, and this means that quantum mechanical approaches solving coupled light-matter problems have to determine the wave functions in each photon subspace, which might be a difficult task.

This approach can be extended to many photon modes and the only limitation is the dimension of the Hamiltonian matrix. As this matrix is very sparse, one can easily diagonalize it even for very large matrices.

As there are only very few light-matter coupled systems with analytical solutions, the present work might be useful to test and develop efficient approximations.

A similar approach can be used for a larger electron number, but then the relative motion part has to be solved numerically.

ACKNOWLEDGMENTS

This work has been supported by the National Science Foundation (NSF) under Grant No. IRES 1826917.

APPENDIX A: DECOUPLING N_p PHOTON MODES

In the case of N_p photon modes the light coupled center of mass Hamiltonian is

$$H_c = -\frac{1}{2}\frac{\partial^2}{\partial u^2} + \frac{1}{2}\omega_u^2 u^2 + \sum_{i=1}^{N_p}\left(-\frac{1}{2}\frac{\partial^2}{\partial q_i^2} + \frac{1}{2}q_i^2\omega_i^2 - 2\lambda_i\omega_i q_i u\right). \quad \text{(A1)}$$

By introducing $u_i = u\sqrt{N_p}$ and $\omega_{ui} = \omega_u/N_p$ the Hamiltonian becomes

$$H_c = \sum_{i=1}^{N_p}\left(-\frac{1}{2}\frac{\partial^2}{\partial u_i^2} - \frac{1}{2}\frac{\partial^2}{\partial q_i^2} + \frac{1}{2}\omega_u^2 u_i^2\right) + \left(\frac{1}{2}\omega_i^2 q_i^2 - 2\omega_i\lambda_i\sqrt{N_p}u_i q_i\right). \quad \text{(A2)}$$

By introducing the coordinate rotation

$$s_i = u_i\sin(\alpha_i) + q_i\cos(\alpha_i), \quad \text{(A3)}$$

and

$$t_i = -u_i\cos(\alpha_i) + q_i\sin(\alpha_i), \quad \text{(A4)}$$

the coupling terms can be eliminated by choosing

$$\tan(2\alpha_i) = \frac{2\omega_i\lambda_i}{(\omega_u/2)^2 - \omega_i}. \quad \text{(A5)}$$

The Hamiltonian becomes

$$H_c = \sum_{i=1}^{N_p} -\frac{1}{2}\frac{\partial^2}{\partial s_i^2} + \frac{1}{2}\omega_{s_i}^2 s_i^2 - \frac{1}{2}\frac{\partial^2}{\partial t_i^2} + \frac{1}{2}\omega_{t_i}^2 t_i^2, \tag{A6}$$

where

$$\omega_{s_i}^2 = \sin^2(\alpha_i)(\omega_u/2)^2 + \cos^2(\alpha_i)\omega_i^2 - 4\sin(\alpha_i)\cos(\alpha_i)\lambda_i\omega_i, \tag{A7}$$

$$\omega_{t_i}^2 = \cos^2(\alpha_i)(\omega_u/2)^2 + \sin^2(\alpha_i)\omega_i^2 + 4\sin(\alpha_i)\cos(\alpha_i)\lambda_i\omega_i. \tag{A8}$$

APPENDIX B: DIAGONALIZATION WITH N_p PHOTON MODES

Consider the same system as in Sec. II A 2, except that here n_p photons are coupled. Hence, there are $N_p = 2n_p$ photon modes involved.

$$|\vec{n}\rangle = |n_1, n_2, \ldots, n_{N_p}\rangle. \tag{B1}$$

Define the vector Kronecker delta as

$$\delta_{\vec{n}\vec{m}} = \prod_{k=1}^{N_p} \delta_{n_k m_k}, \tag{B2}$$

$$\delta^l_{\vec{n}\vec{m}} = \prod_{k=1,k\neq l}^{N_p} \delta_{n_k m_k}. \tag{B3}$$

It is straightforward to generalize Eq. (2.52)

$$\langle \vec{m}, \phi_i|H|\vec{n}, \phi_j\rangle = \delta_{\vec{m}\vec{n}}\delta_{ij}\left(j+\frac{1}{2}\right)\frac{\omega_u}{2} + \delta_{\vec{m}\vec{n}}\delta_{ij}\sum_{k=1}^{N_p}\left(n_k+\frac{1}{2}\right)\omega_k + \sum_{k=1}^{N_p}\sqrt{\frac{2\omega_k}{\omega_u}}\,\lambda\, D_{n_k m_k} D_{ij}\delta^k_{\vec{n}\vec{m}}. \tag{B4}$$

APPENDIX C: CENTER-OF-MASS MOTION FOR MANY PHOTONS

We assume $N_p = 2n_p$ photon modes, and $\boldsymbol{\lambda_\alpha}$'s are not necessarily isotropic in the x, y directions. Thus, the Hamiltonian becomes

$$H = -\frac{1}{2}\nabla_1^2 + \frac{1}{2}\omega_0^2\mathbf{r}_1^2 - \frac{1}{2}\nabla_2^2 + \frac{1}{2}\omega_0^2\mathbf{r}_2^2 + \frac{z_1 z_2}{|\mathbf{r}_1 - \mathbf{r}_2|} + \frac{1}{2}\sum_{\alpha=0}^{N_p}(z_1\boldsymbol{\lambda}_\alpha\cdot\mathbf{r}_1 + z_2\boldsymbol{\lambda}_\alpha\cdot\mathbf{r}_2)^2. \tag{C1}$$

Still imposing $z_1 = z_2$, the radial part remains unchanged and can be solved by Refs. [19,20,53]. Now we solve the CM part. Equation (2.14) becomes

$$\left[-\frac{1}{2}\nabla_{\mathbf{R}}^2 + \frac{1}{2}\omega_{\mathbf{R}}^2\mathbf{R}^2 + 4\sum_{\alpha=0}^{N_p}(\boldsymbol{\lambda}_\alpha\cdot\mathbf{R})^2\right]\xi(\mathbf{R}) = \eta'\xi(\mathbf{R}). \tag{C2}$$

Suppose $\boldsymbol{\lambda}_\alpha = (\lambda_{\alpha 1}, \lambda_{\alpha 2}, 0)$. We further define

$$\tilde{\lambda}_1 = \sum_{\alpha=0}^{N_p}{\lambda_{\alpha 1}}^2,$$
$$\tilde{\lambda}_2 = \sum_{\alpha=0}^{N_p}{\lambda_{\alpha 2}}^2, \tag{C3}$$
$$\tilde{\lambda}_{12} = \sum_{\alpha=0}^{N_p}\lambda_{\alpha 1}\lambda_{\alpha 2},$$

and Eq. (2.16) and (2.17) now read

$$H_{\mathbf{R}} = -\frac{1}{2}\frac{\partial^2}{\partial X^2} - \frac{1}{2}\frac{\partial^2}{\partial Y^2} + \frac{1}{2}\omega_X^2 X^2 + \frac{1}{2}\omega_Y^2 Y^2 + \frac{1}{2}\omega_{XY}XY, \tag{C4}$$

where

$$\omega_X^2 = \omega_{\mathbf{R}}^2 + 8\tilde{\lambda}_1,$$
$$\omega_Y^2 = \omega_{\mathbf{R}}^2 + 8\tilde{\lambda}_2, \tag{C5}$$
$$\omega_{XY} = 16\tilde{\lambda}_{12}.$$

This linearly coupled Hamiltonian can be easily decoupled with the following unitary transformation:

$$U = \frac{1}{(1-ab)^{1/2}}(X + aY),$$
$$V = \frac{1}{(1-ab)^{1/2}}(bX + Y), \tag{C6}$$

where

$$a = \frac{(\tilde{\lambda}_1 - \tilde{\lambda}_2) + \sqrt{(\tilde{\lambda}_1 - \tilde{\lambda}_2)^2 + 4\tilde{\lambda}_{12}^2}}{2\tilde{\lambda}_{12}},$$
$$b = -\frac{(\tilde{\lambda}_1 - \tilde{\lambda}_2) + \sqrt{(\tilde{\lambda}_1 - \tilde{\lambda}_2)^2 + 4\tilde{\lambda}_{12}^2}}{2\tilde{\lambda}_{12}}. \tag{C7}$$

In this case, the decoupled Hamiltonian reads

$$H_R(U,V) = -\frac{1}{2}\frac{\partial^2}{\partial U^2} - \frac{1}{2}\frac{\partial^2}{\partial V^2} + \frac{1}{2}\omega_U^2 U^2 + \frac{1}{2}\omega_V^2 V^2, \tag{C8}$$

where

$$\omega_U = \sqrt{\omega_R^2 + 4(\tilde{\lambda}_1 + \tilde{\lambda}_2) + 4\sqrt{(\tilde{\lambda}_1 - \tilde{\lambda}_2)^2 + 4\tilde{\lambda}_{12}^2}},$$
$$\omega_V = \sqrt{\omega_R^2 + 4(\tilde{\lambda}_1 + \tilde{\lambda}_2) - 4\sqrt{(\tilde{\lambda}_1 - \tilde{\lambda}_2)^2 + 4\tilde{\lambda}_{12}^2}}. \tag{C9}$$

Same as in Eq. (2.19), this is just the Hamiltonian for two noninteracting harmonic oscillators. Hence, the energies for the CM part are

$$\eta = \tfrac{1}{2}\eta' = \tfrac{1}{2}(n_U + \tfrac{1}{2})\omega_U + \tfrac{1}{2}(n_V + \tfrac{1}{2})\omega_V\,,\ n_U,\ n_V = 0, 1, 2\ldots \tag{C10}$$

and the ground state energy is

$$\eta_0 = \tfrac{1}{4}(\omega_U + \omega_V). \tag{C11}$$

Finally, the corresponding wave function is just the product of that of the two independent harmonic oscillators.

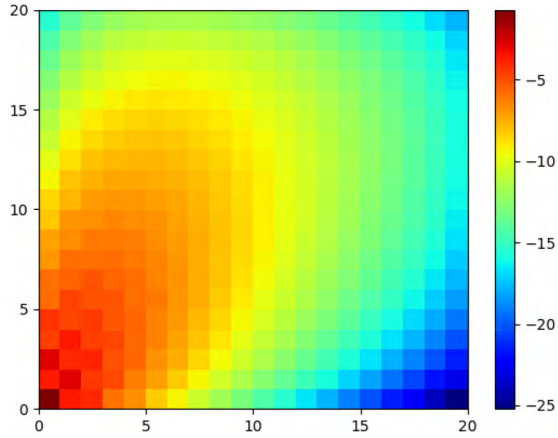

FIG. 6. The logarithm of the occupation numbers in case of two the photon modes. The photon frequencies are ω and 2ω. The coupling vectors are $\boldsymbol{\lambda}$ and $-\boldsymbol{\lambda}$. The vertical axis is the photon number for ω, the horizontal axis is the photon number for 2ω ($\omega_0 = 1$ a.u., $\omega = 1$ a.u., $\lambda = 1$ a.u.).

APPENDIX D: TWO-PHOTON MODE EXAMPLES

The calculation can be extended to many photon modes as it is shown in Appendix B. In this Appendix we show examples of two-photon mode calculations in Figs. 6 and 7. In particular, Fig. 6 shows the photon occupation numbers for the two-photon modes, ω and 2ω. The occupation probability tilts toward the ω axis, showing that the ω modes have higher probabilities than the 2ω ones. Figure 7 is the same calculation as is shown in Fig. 3(a), but with two-photon modes. Overall, the two figures are very similar. The two-photon case reaches higher energies and there are more level crossings. This is because some of the states shown in Fig. 7 are 2ω states and move higher faster. Increasing the number of photon modes helps to reach higher j states and multiphoton modes might be a way to select higher j states or single out a desired j value.

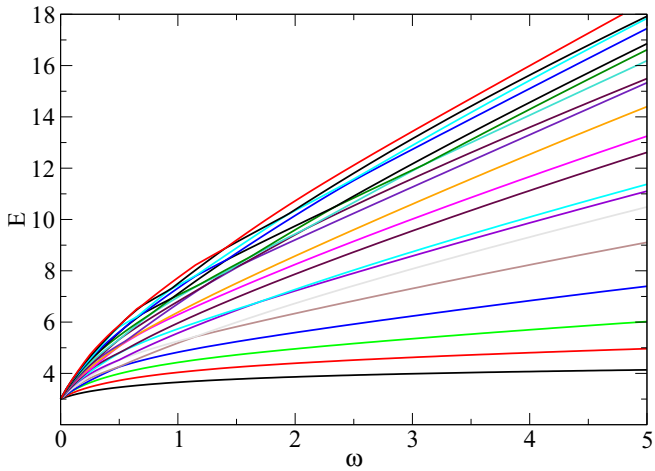

FIG. 7. Energy levels as a function of ω for the two-photon modes. The photon frequencies are ω and 2ω, the coupling vectors are $\boldsymbol{\lambda}$ and $-\boldsymbol{\lambda}$, with $\lambda = \sqrt{\omega}$ ($\omega_0 = 1$ a.u.)

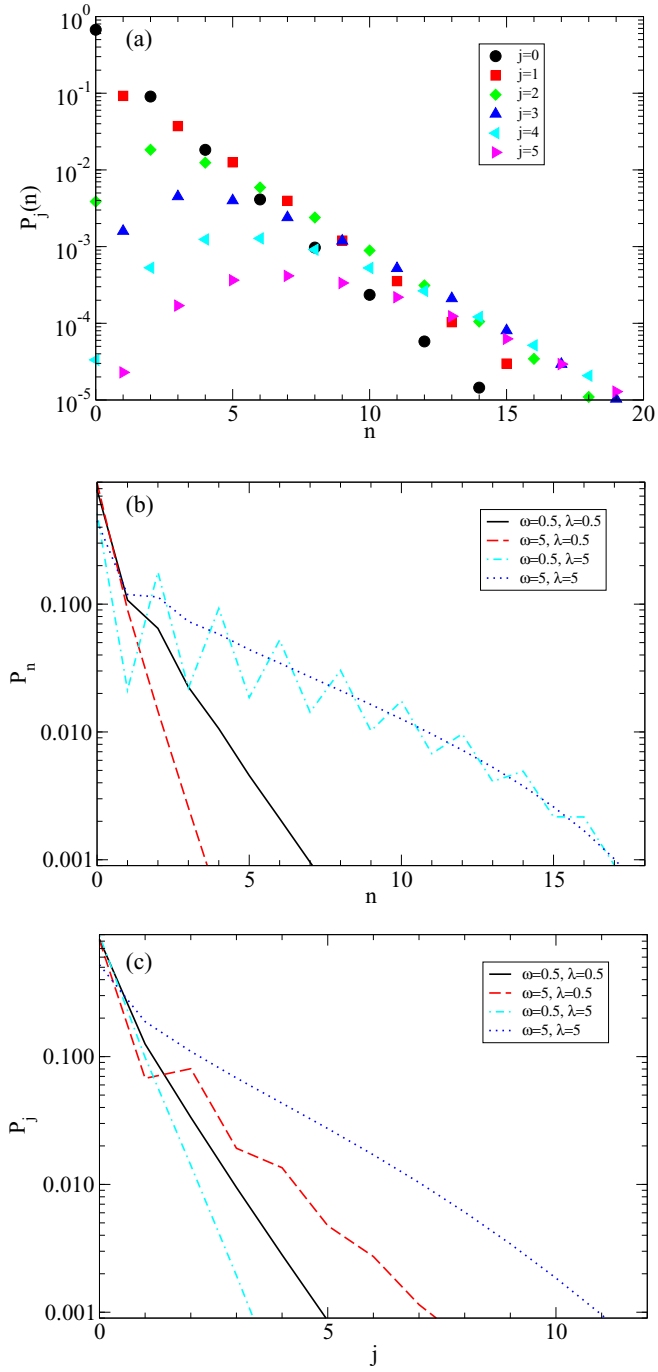

FIG. 8. (a) Probability of the occupation of a jn subspace ($\lambda = 0.5$ a.u. and $\omega = 0.5$ a.u.), $P_j(n)$. (b) $P_n = \sum_j P_n(j)$. (c) $P_j = \sum_n P_n(j)$. $\omega_0 = 1/3$ a.u. is used in the calculations.

APPENDIX E: DECOMPOSITION IN DIFFERENT SPATIAL AND PHOTON SPACES

The total wave function will be a linear combination of the $\phi(\mathbf{r})\psi_j(\mathbf{R})|n\rangle$ components. The probability of a given component is given by

$$P_j(n) = |c^0_{jn}|^2 \tag{E1}$$

and depends on ω_0, ω and λ. An example for $P_j(n)$ is given in Fig. 8(a). First, we note that due to the structure in Eq. (2.52),

the probabilities follow a checkerboardlike structure: odd photon numbers couple to odd j and even photon numbers couple to even j. The probabilities decrease for large photon numbers. The low CM excitations, $j = 0, 1, 3$, are the most dominant terms for low photon numbers. The probability of the higher CM excitations ($j = 2, 3, 4, 5$) first increases with the photon number, then reaches a maximum and starts to decrease.

Figure 8(b) shows the sum $P_n = \sum_j P_n(j)$. By increasing λ, the higher photon spaces are coupled and the occupation of lower photon numbers increases. However, the effect of ω is more complicated. The coupling increases as $\sqrt{\omega}$ but with larger photon frequency the photon harmonic oscillator states move higher in energy ($n\hbar\omega$) and their occupation decreases. This latter effect seems to be dominant for smaller λ. In Fig. 8(b), in the case of $\lambda = 0.5$ a.u., P_n is the same for $n = 0, 1$ for $\omega = 0.5$ a.u. and $\omega = 5$ a.u., but for higher n, P_n is much smaller for $\omega = 5$ a.u. For higher λ values this effect becomes less important. The oscillations (the even states have higher occupation than the odd states) in the case of $\omega = 0.5$, $\lambda = 5$ a.u. always appear when ω is much smaller than λ and probably due to the checkerboardlike coupling.

Figure 8(c) shows the sum $P_j = \sum_n P_n(j)$. By increasing ω, the occupations of the low photon number states decrease and the occupations of the higher states increase. Increasing λ increases ω_u and pushes the CM states higher, and those states do not couple with the low j sector, so increasing λ decreases P_j. The effect of λ is similar to ω in the previous case: λ increases the coupling, but larger λ means larger ω_u and the CM states are pushed higher. For low ω, increasing λ relaxes the occupation, but for large ω, the coupling dominates and the λ increases the occupation of the higher n states.

[1] F. Buchholz, I. Theophilou, S. E. B. Nielsen, M. Ruggenthaler, and A. Rubio, ACS Photonics **6**, 2694 (2019).
[2] C. Schäfer, M. Ruggenthaler, H. Appel, and A. Rubio, Proc. Natl. Acad. Sci. **116**, 4883 (2019).
[3] M. Ruggenthaler, N. Tancogne-Dejean, J. Flick, H. Appel, and A. Rubio, Nat. Rev. Chem. **2**, 0118 (2018).
[4] J. Flick, M. Ruggenthaler, H. Appel, and A. Rubio, Proc. Natl. Acad. Sci. **112**, 15285 (2015).
[5] J. Flick, M. Ruggenthaler, H. Appel, and A. Rubio, Proc. Natl. Acad. Sci. **114**, 3026 (2017).
[6] V. Rokaj, D. M. Welakuh, M. Ruggenthaler, and A. Rubio, J. Phys. B **51**, 034005 (2018).
[7] N. Rivera, J. Flick, and P. Narang, Phys. Rev. Lett. **122**, 193603 (2019).
[8] J. Flick and P. Narang, Phys. Rev. Lett. **121**, 113002 (2018).
[9] N. M. Hoffmann, L. Lacombe, A. Rubio, and N. T. Maitra, J. Chem. Phys. **153**, 104103 (2020).
[10] I. V. Tokatly, Phys. Rev. B **98**, 235123 (2018).
[11] J. Galego, F. J. Garcia-Vidal, and J. Feist, Phys. Rev. Lett. **119**, 136001 (2017).
[12] A. Mandal, S. Montillo Vega, and P. Huo, J. Phys. Chem. Lett. **11**, 9215 (2020).
[13] L. S. Cederbaum and A. I. Kuleff, Nat. Commun. **12**, 4083 (2021).
[14] T. Szidarovszky, G. J. Halász, A. G. Császár, L. S. Cederbaum, and A. Vibók, J. Phys. Chem. Lett. **9**, 6215 (2018).
[15] Y. Ashida, A. İmamoğlu, and E. Demler, Phys. Rev. Lett. **126**, 153603 (2021).
[16] N. Rivera and I. Kaminer, Nat. Rev. Phys. **2**, 538 (2020).
[17] A. Le Boité, Adv. Quantum Technol. **3**, 1900140 (2020).
[18] F. J. Garcia-Vidal, C. Ciuti, and T. W. Ebbesen, Science **373**, eabd0336 (2021).
[19] M. Taut, Phys. Rev. A **48**, 3561 (1993).
[20] M. Taut, J. Phys. A **27**, 1045 (1994).
[21] M. Taut, J. Phys. A **28**, 2081 (1995).
[22] J. Karwowski and G. Pestka, Theor. Chem. Acc. **118**, 519 (2007).
[23] V. M. Villalba and R. Pino, Phys. Lett. A **238**, 49 (1998).
[24] J. Karwowski, J. Phys.: Conf. Ser. **104**, 012033 (2008).
[25] A. Turbiner, Commun. Math. Phys. **118**, 467 (1988).
[26] L. Liu and Q. Hao, Theor. Math. Phys. **183**, 730 (2015).
[27] C. A. Downing and M. E. Portnoi, Phys. Rev. B **94**, 045430 (2016).
[28] C.-L. Ho and V. R. Khalilov, Phys. Rev. A **61**, 032104 (2000).
[29] C.-M. Chiang and C.-L. Ho, J. Math. Phys. **43**, 43 (2002).
[30] D. Agboola and Y.-Z. Zhang, Mod. Phys. Lett. A **27**, 1250112 (2012).
[31] J. Karwowski and H. A. Witek, Mol. Phys. **114**, 932 (2016).
[32] K. Akhmedov and N. Guseinova, Russ. Phys. J. **52**, 321 (2009).
[33] F. M. Pont, O. Osenda, and P. Serra, J. Phys. A **51**, 195303 (2018).
[34] C. A. Downing, Phys. Rev. A **95**, 022105 (2017).
[35] P.-F. Loos and P. M. W. Gill, Phys. Rev. Lett. **108**, 083002 (2012).
[36] G.-J. Guo, Z.-Z. Ren, B. Zhou, and X.-Y. Guo, Int. J. Mod. Phys. B **26**, 1250201 (2012).
[37] P.-F. Loos and P. M. W. Gill, Phys. Rev. Lett. **103**, 123008 (2009).
[38] P.-F. Loos and P. M. W. Gill, Mol. Phys. **108**, 2527 (2010).
[39] R. Jestädt, M. Ruggenthaler, M. J. T. Oliveira, A. Rubio, and H. Appel, Adv. Phys. **68**, 225 (2019).
[40] A. Frisk Kockum, A. Miranowicz, S. De Liberato, S. Savasta, and F. Nori, Nat. Rev. Phys. **1**, 19 (2019).
[41] C. Schäfer, M. Ruggenthaler, and A. Rubio, Phys. Rev. A **98**, 043801 (2018).
[42] J. Flick, C. Schäfer, M. Ruggenthaler, H. Appel, and A. Rubio, ACS Photonics **5**, 992 (2018).
[43] D. Sidler, M. Ruggenthaler, H. Appel, and A. Rubio, J. Phys. Chem. Lett. **11**, 7525 (2020).
[44] L. Lacombe, N. M. Hoffmann, and N. T. Maitra, Phys. Rev. Lett. **123**, 083201 (2019).
[45] G. M. Andolina, F. M. D. Pellegrino, V. Giovannetti, A. H. MacDonald, and M. Polini, Phys. Rev. B **100**, 121109 (2019).
[46] M. Schuler, D. D. Bernardis, A. M. Läuchli, and P. Rabl, SciPost Phys. **9**, 66 (2020).
[47] A. Settineri, O. Di Stefano, D. Zueco, S. Hughes, S. Savasta, and F. Nori, Phys. Rev. Research **3**, 023079 (2021).
[48] V. Rokaj, M. Ruggenthaler, F. G. Eich, and A. Rubio, arXiv:2006.09236.

[49] S. Shin and H. Metiu, J. Chem. Phys. **102**, 9285 (1995).
[50] A. Mandal, T. D. Krauss, and P. Huo, J. Phys. Chem. B **124**, 6321 (2020).
[51] E. A. Power, S. Zienau, and H. S. W. Massey, Philos. Trans. R. Soc. London A **251**, 427 (1959).
[52] M. Ruggenthaler, J. Flick, C. Pellegrini, H. Appel, I. V. Tokatly, and A. Rubio, Phys. Rev. A **90**, 012508 (2014).
[53] See Supplemental Material at http://link.aps.org/supplemental/10.1103/PhysRevB.104.165147 for additional examples.
[54] We thank the anonymous referee for pointing us in this direction.